

## ERROR EFFECTS IN MICROLASER SENSORS

**W. Holzapfel, L. Hou, and S. Neuschaefer-Rube**

University of Kassel, Institute for Measurement and Automation  
D-34109 Kassel, Germany

*Abstract: Microlaser sensors use the intracavity photoelastic effect in Nd:YAG-laser crystals to detect force and force-related quantities like torque, pressure and inertial acceleration. Error effects are caused by local and temporal temperature changes as well as by nonlinear influences of the laser crystal, its support and the load system. Measurement resolution is limited by seismic noise and non-reproducibility. We have achieved a low relative temperature coefficient of  $10^{-6}/^{\circ}\text{C}$  and a relative reproducibility of  $10^{-5}$  related to a maximum input load of 100 N. These results are advantageous properties compared with some competing force sensors.*

*Keywords: Force Measurement, Photoelastic Effect, Microlaser*

### 1 INTRODUCTION

Microlasers using the resonator-internal photoelastic effect in active laser crystals are very suitable to detect precisely mechanical magnitudes like forces, torques, pressures and inertial accelerations. In previous investigations we could demonstrate experimentally a measurement range of 9 decades for the force  $F$  and a maximum load of 100 N covered by each single sensor (e. g. [1]). If there is no static but a time-dependent input force, the dynamic behavior of the mechanical measurement setup must be taken into consideration. The resonator-internal measurement effect itself does not change its sensitivity for sinusoidal forces  $F$  at frequencies from DC up to at least 100 kHz [1].

Output signal of the microlaser sensor is the optical beat frequency  $f$  of two orthogonally polarized laser modes. This frequency depends on the optical birefringence in the crystal caused by the photoelastic effect. The birefringence is a consequence of internal mechanical stresses induced by the input signal. Up to now, the application of the measurement procedure to measure forces in a fixed direction perpendicular to the resonator axis was investigated thoroughly (e.g. [1]). For this purpose, a cylindrical Nd:YAG laser crystal lying on a support is loaded via a load system (Fig. 1a).

Due to the vertical stiffnesses  $C_C$ ,  $C_L$  of the crystal and the load system, the force  $F^*$  acts on the crystal (Fig. 1b). The mechanical stresses induced by this force lead to a resonator-internal optical phase difference  $D_F$ . By this, the beat frequency  $f$  changes in dependence of  $F^*$ .

$$\Delta F = \frac{360^{\circ} \cdot C_0 \cdot L}{\lambda} \cdot (\sigma_1 - \sigma_2), \quad \Delta f = \frac{\Delta F}{180^{\circ}} \cdot \frac{c}{2 \cdot n_0 \cdot L} = \frac{\nu_0 \cdot C_0 \cdot G}{n_0 \cdot L \cdot d} \cdot F^* = S \cdot F^* \quad (1a, b)$$

( $C_0$ : photoelastic constant,  $(\sigma_1 - \sigma_2)$ : difference of the principal stresses,  $L$ : crystal length,  $\lambda$ : laser wavelength,  $c$ : velocity of light,  $n_0$ : Refraction index of the crystal,  $\nu_0$ : light frequency,  $G$ : geometry factor depending on the geometry of crystal and support,  $d$ : diameter of the laser crystal,  $S$ : sensitivity). Precondition for the proportionality  $Df \sim F^*$  in Eq. (1b) is a correctly adjusted offset phase difference. This will be explained in Chapter 2. Using Nd:YAG crystals with the dimensions  $\varnothing 3 \text{ mm} \times 5 \text{ mm}$  and a plane support, in the case of central irradiation and  $F = F^*$ , a sensitivity  $S = 32.9 \text{ MHz/N}$  results.

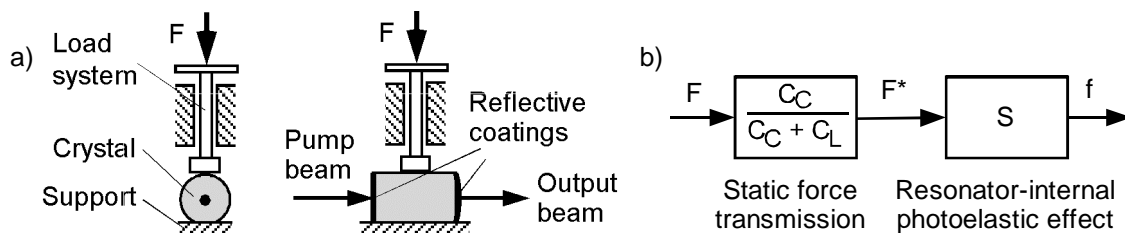


**Figure 1.** Nd:YAG laser with load system and plane support: **a)** mechanical setup, **b)** signal flow.

Until now the microlaser sensor has been tested by means of experimental setups only. Because of the very advantageous properties of the sensor the measurement principle seems suitable to be

transformed into industrial applications. For this purpose, an investigation of the major error effects is necessary.

## 2 ERROR EFFECTS CAUSED BY THE CRYSTAL

The unloaded laser crystal is tested in [2]. It turns out that variations in temperature cause the biggest errors. Absolute temperature as well as its temporal derivative influence the beat frequency. Every single crystal has its own individual temperature behavior. Temperature coefficients of the beat frequency  $f$  below 3 kHz/°C can be achieved by compensating measures. For an upper limit of the measurement range of 100 N [1], this corresponds to a relative error of  $10^{-6}/^{\circ}\text{C}$ .

In the following we will discuss additional error effects caused by the loading of the sensor. For the loaded crystal, the load-induced phase difference  $D_F$  depends on the photoelastic constant  $C_0$  (see Eq. (1)). This constant is influenced by the crystal class and the cut of the crystal. The Nd:YAG crystals proven as microlaser sensors belong to the class of cubic crystals and are cut in the [111]-direction. In this case the photoelastic constant  $C_0 = C_{111}$  can be calculated from

$$C_{111} = \frac{1}{6} \cdot n_0^3 \cdot [(p_{11} - p_{12}) \cdot (s_{11} - s_{12}) + 2 \cdot p_{44} \cdot s_{44}] \quad (2)$$

( $n_0$ : refraction index,  $p_{ij}$ : elasto-optic coefficients,  $s_{ij}$ : stiffnesses). The photoelastic constant  $C_{111}$  is independent of the direction of the principal stresses. For YAG, the values for  $n_0$ ,  $p_{ij}$  and  $s_{ij}$  are [3]:

$$n_0 = 1.82, p_{11} = -0.029, p_{12} = 0.0091, p_{44} = -0.0615, \\ s_{11} = 3.60 \cdot 10^{-6} \text{ mm}^2/\text{N}, s_{12} = -0.91 \cdot 10^{-6} \text{ mm}^2/\text{N}, s_{44} = 8.73 \cdot 10^{-6} \text{ mm}^2/\text{N}$$

Inserting these values in Eq. (2) yields  $C_{111} = 1.25 \cdot 10^{-6} \text{ mm}^2/\text{N}$ .

We carried out x-ray tests of laser crystals. These tests have shown that the actual irradiation direction deviates from the [111]-direction by the deviation angle  $\chi$ . These deviations are caused by the production process of the crystals. Measurements on different crystals turned out  $\chi$ -values between  $0.32^{\circ}$  and  $1.49^{\circ}$ . This leads to changes in the photoelastic constant  $C_0$ . Additionally for  $c \neq 0$ ,  $C_0$  depends on the rotation angle  $\theta$ , i.e. the azimuth of the principal stress direction to the crystal axes. For  $\chi = 1.49^{\circ}$ , maximum changes in the photoelastic constant of approximately 5% occur.

Furthermore, YAG crystals cut in the [100]-direction are commercially available. For these crystals the photoelastic constant  $C_0 = C_{100}$  is

$$C_{100} = \frac{1}{2} \cdot n_0^3 \cdot \sqrt{(p_{11} - p_{12})^2 \cdot (s_{11} - s_{12})^2 \cdot \cos^2 2\theta + p_{44}^2 \cdot s_{44}^2 \cdot \sin^2 2\theta}, \quad (3)$$

i.e. there is a strong dependence of the photoelastic constant on the principal stress direction  $\theta$ . A rotation of the crystal around the irradiation axis results in a significant change in the sensitivity of the microlaser sensor. Taking the values of  $n_0$ ,  $p_{ij}$ , and  $s_{ij}$  for YAG into account, Eq. (3) yields values for  $C_{100}$  between  $0.52 \cdot 10^{-6} \text{ mm}^2/\text{N}$  ( $\theta = 0^{\circ}, \pm 90^{\circ}, 180^{\circ}$ ) and  $1.62 \cdot 10^{-6} \text{ mm}^2/\text{N}$  ( $\theta = \pm 45^{\circ}, \pm 135^{\circ}$ ).

Even without load, there is generally an offset phase difference  $\varphi_0$  in the laser crystal. In analogy to Eq. (1b), the offset phase difference  $\varphi_0$  is proportional to the offset beat frequency  $f_0$ :

$$f_0 = \frac{\Delta_0}{180^{\circ}} \cdot \frac{c}{2 \cdot n_0 \cdot L} \quad (4)$$

The offset phase difference superposes nonlinearly with the load-induced phase difference  $\varphi_F$ . The resulting phase difference  $D$  depends on the difference ( $\varphi_0 - \varphi_F$ ) of the main-axis orientations of the phase differences  $D_0$  and  $D_F$  [4]. The resulting phase difference leads to a resulting beat frequency  $f$ . This beat frequency is given by

$$f = \sqrt{f_0^2 + \Delta f^2 + 2 \cdot f_0 \cdot \Delta f \cdot \cos[2 \cdot (\varphi_0 - \varphi_F)]} \quad (5)$$

Fig. 2 shows the beat frequency  $f$  in dependence on the force  $F$  for different values of the parameter  $\varphi_0 - \varphi_F$  calculated with Eq. (5). The theoretical sensitivity  $S = 32.9 \text{ MHz/N}$  of a crystal with the dimensions  $\varnothing 3 \text{ mm} \times 5 \text{ mm}$  lying on a plane support and a typical offset beat frequency  $f_0 = 16 \text{ MHz}$  are used.

For  $(\varphi_0 - \varphi_F) = 0^\circ$  and  $90^\circ$ , resp., linear superposition  $f = f_0 + Df$  and  $f = |f_0 - Df|$ , resp., is valid. To achieve the linear measurement equation  $Df(F^*)$  represented in Eq. (1b), one of these two cases has to be realized. Otherwise, there is a nonlinear sensor characteristic  $Df(F)$  especially for small forces.

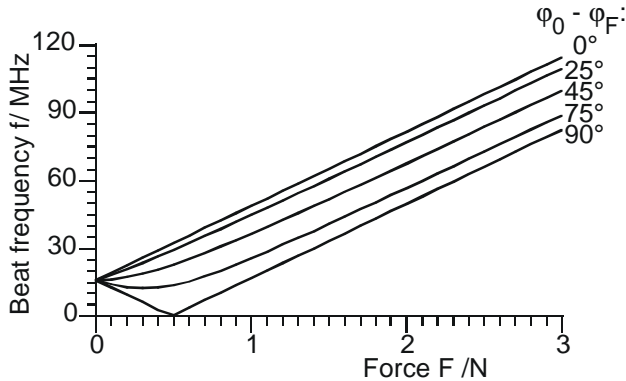


**Figure 2.** Dependence of the beat frequency  $f$  on the crystal load  $F = F^*$  for different main-axis orientations  $\varphi_0 - \varphi_F$  (offset beat frequency  $f_0 = 16$  MHz, sensitivity  $S = 32.9$  MHz/N).

### 3 ERRORS CAUSED BY LOAD SYSTEM AND SUPPORT

Load system and support of the microlaser sensor can significantly influence the errors of the sensor. Major task of the load system is to isolate the crystal from horizontal forces as well as from bending and torsional moments. We tested three different principles of load systems (Fig. 3). Parallel-guided load systems (Fig. 3a) are used e.g. in scales with electromagnetic force compensation. In such a load system a vertical displacement also causes a horizontal displacement. This is avoided by a symmetrical load system with slitted leaf springs (Fig. 3b). In a load system shown in Fig. 3c, a high-quality ball bearing is used to realize a small vertical stiffness  $C_L$ .

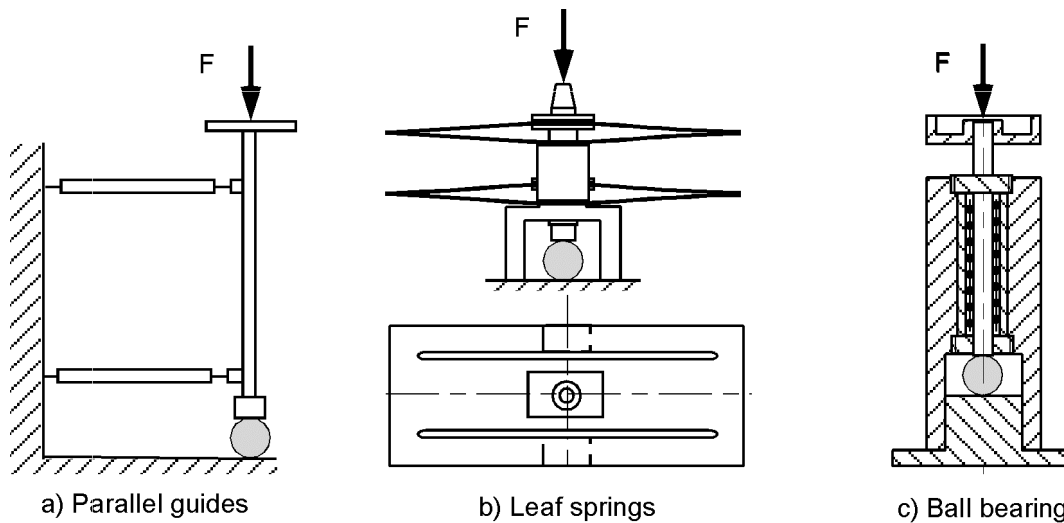


**Figure 3.** Tested types of load systems.

We determined the characteristic of the microlaser sensor with the different load systems shown in Fig. 3. Test masses  $m$  are successively applied to and successively removed from the load system. Nd:YAG crystals with dimensions  $\varnothing 3 \text{ mm} \times 5 \text{ mm}$  and a plane support in combination with one of the load systems shown in Fig. 3 are used. Fig. 4a shows the dependence of the measured beat frequency  $f$  on the applied weighing force  $F$  and the linear approximation following from the least square method. In Fig. 4b the deviations  $Df$  of the measured points from the approximated linear characteristic are shown.

All load systems lead to linear characteristics with nearly identical sensitivities. The calculated values are  $S_1=30.9$  MHz/N (parallel guides),  $S_2=31.6$  MHz/N (leaf springs) and  $29.3$  MHz/N (ball bearing). All these sensitivities are slightly smaller than the theoretical value of  $32.9$  MHz/N. This can be explained by non-central irradiation of the crystal and the vertical stiffness  $C_L > 0$  of the load systems, resp. The different offsets  $Df_0$  of the beat frequency are caused by different offset loads of the load

system. The parallel-guided load system and the load system with ball bearing have significantly less deviations  $Df$  from the linear characteristic than the load system with leaf springs. The rms values of the deviations are 84 kHz (parallel guides) and 145 kHz (ball bearing) and 1.95 MHz (leaf springs). Taking the sensitivities into account, this corresponds to force values of 2.7 mN, 4.5 mN and 66.6 mN, resp.

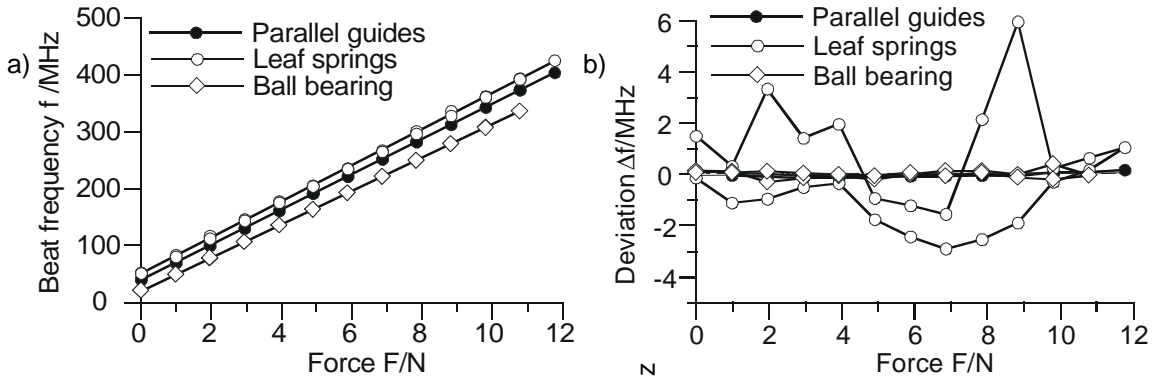


**Figure 4.** a) Characteristic of the microlaser sensor using different load systems (plane support, crystal dimensions  $\varnothing 3 \text{ mm} \times 5 \text{ mm}$ )  
b) Deviation of the measured points in a) from the linear characteristic.

In order to determine the temperature behavior of the load systems, the beat frequency  $f$  of the microlaser sensor is measured during a (small-scale) linear increase and a following decrease of the temperature  $T$ .  $T$  is near room temperature. The determined changes  $Df$  in the beat frequency at temperature changes  $DT$  are shown in Fig. 5. A weighing force of a mass  $m = 600 \text{ g}$  was applied to the load system and a plane support was used. No compensation measures are employed.

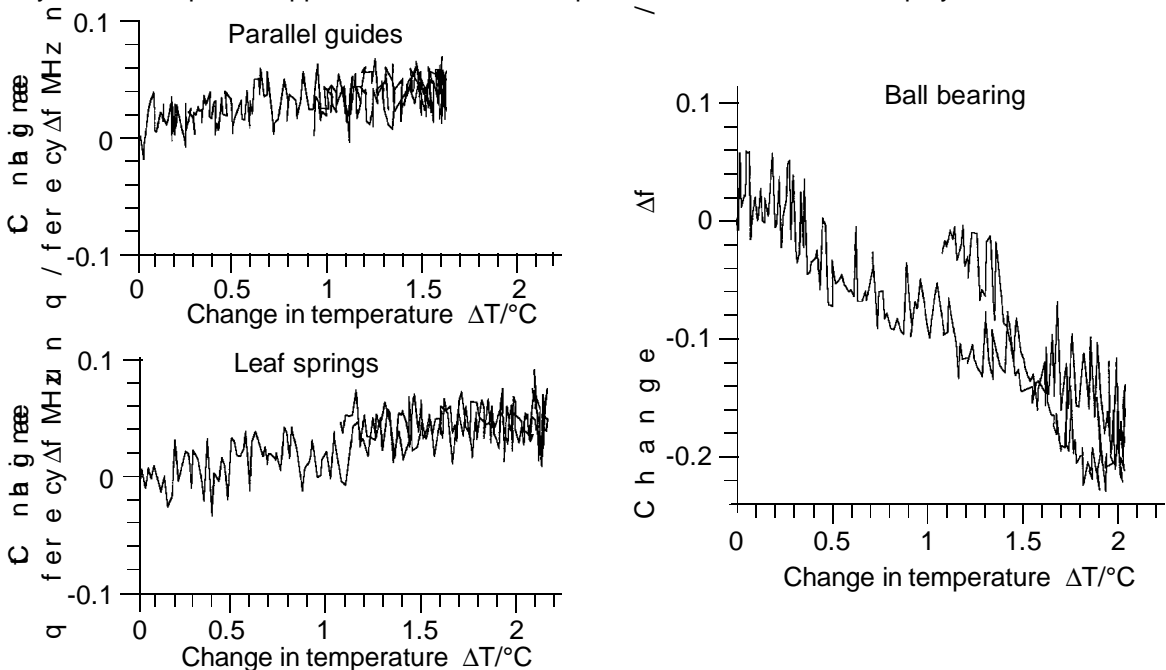


**Figure 5.** Dependence of beat frequency  $f$  on small scale temperature changes  $T$  for different load systems (plane support, force  $F = 5.89 \text{ N}$ ).

Fig. 5 demonstrate the superior behavior of the load systems with parallel guides and leaf springs. Using these load systems, the temperature-caused drift is overlapped considerably by seismic noise. From the measurement using the ball bearing, a temperature coefficient  $df/dT = 100 \text{ kHz}/^\circ\text{C}$  can be calculated. Using the parallel guides or the leaf springs with temperature changes, the loaded crystal behaves nearly like the unloaded crystal. For the unloaded crystal a temperature coefficient of  $df/dT = 5 \text{ kHz}/^\circ\text{C}$  was found. Further measurements with various forces  $0 \text{ N} \leq F \leq 5.89 \text{ N}$  do not show any dependence of the temperature coefficient on the load  $F$ . We have no indication for a different

behavior at higher loads. Therefore we conclude that it is allowed to calculate a relative temperature coefficient using the maximum load of 100 N. Relating  $df/dt$  to  $F = 100$  N, a value of  $1.6 \cdot 10^{-6}$  results.

From the determination of the characteristics (Fig. 4) follows an advantageous behavior of the load systems with parallel guides and with ball bearings. However, the load system with ball bearing yields a significant increase in the temperature coefficient in comparison to the unloaded crystal. Therefore, the parallel-guided load system should be preferred.

In Fig. 3 to 5, the load systems were combined with a plane support. In order to fix the position of the crystal, we tested supports which have the form of a v-groove with the groove angle  $\alpha$  (Fig. 6a). The normal force  $N$  and the friction force  $\mu \cdot N$  act at the two contact points between crystal and support. The special case  $\alpha=0$  of the v-groove is the plane support. In this case no friction can occur.

The geometry factor  $G$  in Eq. (1) depends on the groove angle  $\alpha$ , the friction coefficient  $\mu$  and the irradiation point  $P(r, \gamma)$ . An increasing groove angle  $\alpha$  always reduces the geometry factor  $G$  and therefore the sensitivity  $S$  of the microlaser sensor (Fig. 6b).

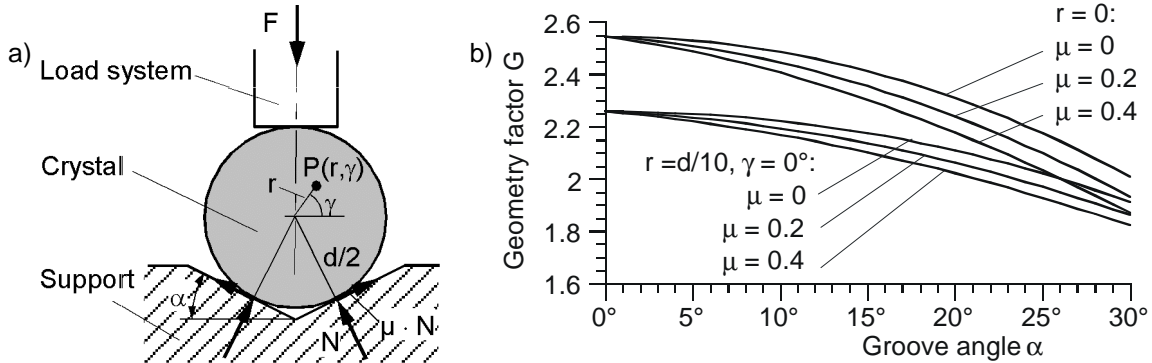


**Figure 6.** a) Loaded crystal in a v-groove ( $N$ : Normal force,  $\mu$ : friction coefficient),  
b) Dependence of the geometry factor  $G$  on the groove angle  $\alpha$  for different friction coefficients  $\mu$  and positions of the point  $P$ .

In the case of central irradiation of the crystal ( $r = 0$ ), the geometry factor  $G$  is

$$G = \frac{4}{\pi} \cdot \frac{\cos \alpha + \cos 2\alpha + \mu \cdot \sin \alpha}{\cos \alpha + \mu \cdot \sin \alpha} \quad (6)$$

For a plane support ( $\alpha = 0^\circ$ )  $G = 8/\pi$  results.

We experimentally compared a plane support and a v-groove with  $\alpha = 20^\circ$ . First we determined the characteristics of the microlaser sensor using the parallel-guided load system, a crystal with the dimensions  $\varnothing 3$  mm  $\times$  5 mm and the two different supports (Fig. 7).

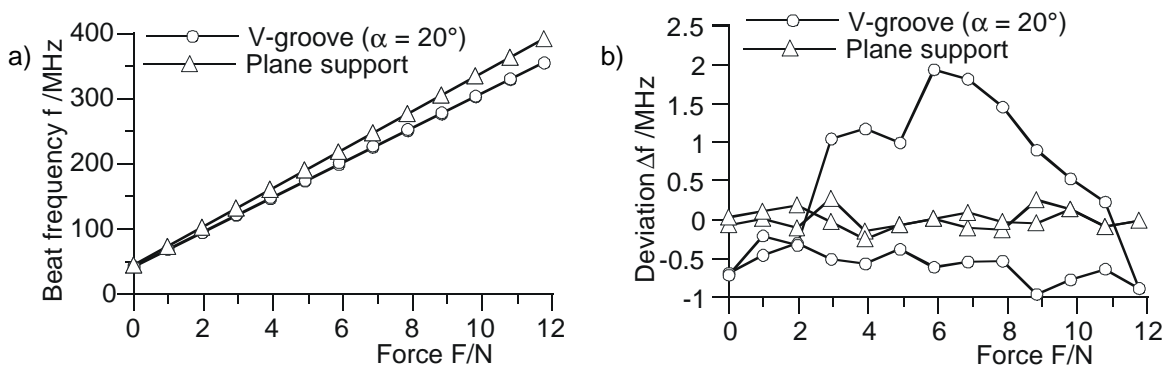


**Figure 7.** a) Characteristic of the microlaser sensor using different supports (parallel-guided load system, crystal dimensions  $\varnothing 3$  mm  $\times$  5 mm),  
b) Deviation of the measured points in a) from the linear characteristic.

The measured beat frequencies and the linear approximation (Fig. 7a) show an identical offset  $f_0$  but different sensitivities. The linear approximation yields sensitivities  $S_1 = 29.48$  MHz/N (plane support) and  $S_2 = 26.60$  MHz/N (v-groove), i.e.  $S_1/S_2 = 1.1083$ . The exact values of  $r, \gamma$  of the crystal's irradiation point  $P$  are not known. For  $r = 0$ , from Eq. (6), a theoretical value of  $S_1/S_2 = 1.1080$  for  $\mu = 0.2$  would result. The deviations of the measured points from the linear approximation are shown in Fig. 7b. Rms-values of 125 kHz for the plane support and 885 kHz for the v-groove follow from the measured points. This corresponds to the force deviations 4.2 mN and 33.2 mN, resp.

Analog to the comparison of different load systems, we investigated the temperature dependence of the beat frequency when different supports are used. As before, a linear increase of temperature followed by a linear decrease is used as the temperature test signal. In analogy to Fig. 5, a weighing force  $F = 5.89 \text{ N}$  was applied to the parallel-guided load system. Fig. 8 shows the dependence of the beat frequency  $f$  on the temperature  $T$ . There is a significantly lower dependence of the beat frequency on the temperature if a plane support is used.

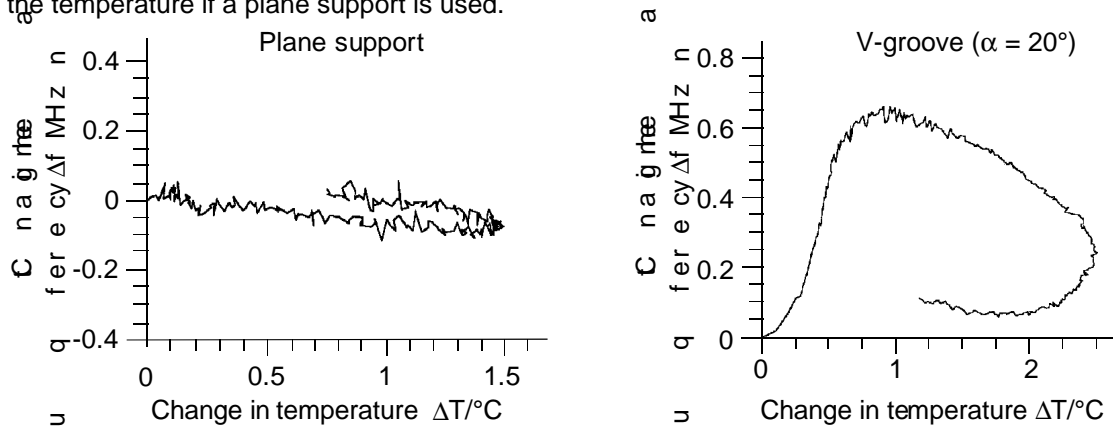


**Figure 8.** Dependence of beat frequency  $f$  on small scale temperature changes  $\Delta T$  for different supports (parallel-guided load system, Force  $F = 5.89 \text{ N}$ ).

#### 4 MEASUREMENT REPRODUCIBILITY

To determine the reproducibility, multiple loadings and unloadings were carried out. Here a parallel-guided load system combined with a plane support was applied. Standard deviations of 73 kHz (force  $F=1 \text{ N}$ ) and 37 kHz (force  $F=3 \text{ N}$ ) were determined. This corresponds to changes in DF of 2.4 mN and 1.2 mN, resp. In reference to a measurement range of 100 N, the relative reproducibility was about  $10^{-5}$ .

The measurement is disturbed by seismic influences. On measuring the weight forces, an increasing noise of the beat frequency  $f$  occurs with increasing total load (load system offset plus mass to be measured). With static forces the influence of the seismic noise can be reduced by temporally averaging the beat frequency  $f$ . For dynamic input signals with a given modulation frequency  $f_{\text{mod}}$ , the seismic noise can be widely eliminated by demodulation and following spectral analysis.

#### 5 CONCLUSIONS

In our investigations we found a number of disturbances of the microlaser sensor which systematically influence its offset and its sensitivity. Therefore, they can widely be eliminated by reference measurements. This is true for the error effects of the crystal as well as the different offsets and sensitivities caused by the different load systems and the support. The non-systematical deviations from the linear characteristic and the temperature effects can be minimized by using the parallel-guided load system and a plane support. In our previous investigations on resonator-internal measurement procedures we have already achieved values for reproducibility ( $10^{-5}$ ) and temperature variation ( $10^{-6}/^\circ\text{C}$ ) which are quite advantageous compared with some conventional measurement procedures (e.g. strain gauges [5]). In our opinion the errors can be further diminished by additional optimizing measures.

#### REFERENCES

- [1] W. Holzapfel, M. Kobusch, St. Neuschaefer-Rube, L. Hou, Dynamic Testing of Laser Force Transducers, in: *Proceedings of the IMEKO XV World Congress* (Osaka, Japan, June 13-18, 1999) Vol. III, 159-166.
- [2] St. Neuschaefer-Rube, W. Holzapfel, and L. Hou, Signal properties of monolithic Nd:YAG lasers, in: *Proceedings of the XVI IMEKO World Congress* (Vienna, Austria, September 25-28, 2000).
- [3] Landolt Börnstein, *Numerical Data and Functional Relationships in Science and Technology*, Volume III/11, Springer Verlag, Berlin, 1979.
- [4] W. Holzapfel, St. Neuschaefer-Rube, Measurements of the ellipsometrical parameters of optical components inside an active laser, in: *Proceedings of SPIE* **2873** (1996), 133-136.
- [5] W. Weiler (Ed.), *Handbuch der physikalisch-technischen Kraftmessung*, Vieweg Verlag, Braunschweig, 1993.

**AUTHORS:** W. HOLZAPFEL, L. HOU, and St. NEUSCHAEFER-RUBE, University of Kassel, Institute for Measurement and Automation, D-34109 Kassel, Germany, Phone: ++49 561 8042757/8  
Fax: ++49 561 8042847, E-mail: Holzapfel@imat.maschinenbau.uni-kassel.de